Original Article

Combinatory transplantation of mesenchymal stem cells with flavonoid small molecule in acellular nerve graft promotes sciatic nerve regeneration

Journal of Tissue Engineering
Volume 11: 1–19

DOI: 10.1177/2041731420980136
journals.sagepub.com/home/tej
SAGE

Wen-yuan Li[1†], Hua Jia[2,3†], Zhen-Dong Wang[4], Feng-guo Zhai[5], Guang-da Sun[1], Duo Ma[1], Gui-Bo Liu[1], Chun-Mei Li[6] and Ying Wang[1]

Abstract

Previous animal studies have demonstrated that the flavonoid small-molecule TrkB agonist, 7, 8-dihydroxyflavone (DHF), promotes axon regeneration in transected peripheral nerves. In the present study, we investigated the combined effects of 7, 8-DHF treatment and bone marrow-derived stem/stromal cells (BMSCs) engraftment into acellular nerve allografts (ANAs) and explore relevant mechanisms that may be involved. Our results show that TrkB and downstream ERK1/2 phosphorylation are increased upon 7, 8-DHF treatment compared to the negative control group. Also, 7, 8-DHF promotes proliferation, survival, and Schwann-like cell differentiation of BMSCs in vitro. While selective ERK1/2 inhibitor U0126 suppressed the effect of upregulation of ERK1/2 phosphorylation and decreased cell proliferation, survival, and Schwann-like cell differentiation partially induced by 7, 8-DHF. In vivo, 7, 8-DHF promotes survival of transplanted BMSCs and upregulates axonal growth and myelination in regenerating ANAs. 7, 8-DHF+BMSCs also improved motor endplate density of target musculature. These benefits were associated with increased motor functional recovery. 7, 8-DHF+BMSCs significantly upregulated TrkB and ERK1/2 phosphorylation expression in regenerating ANA, and increased TrkB expression in the lumbar spinal cord. The mechanism of 7, 8-DHF action may be related to its ability to upregulate TrkB signaling, and downstream activation of survival signaling molecules ERK1/2 in the regenerating ANAs and spinal cord and improved survival of transplanted BMSCs. This study provides novel foundational data connecting the benefits of 7, 8-DHF treatment in neural injury and repair to BMSCs biology and function and demonstrates a potential combination approach for the treatment of injured peripheral nerve via nerve graft transplant.

Keywords

7, 8-DHF, BMSCs, axonal regeneration, peripheral nerve injury

Date received: 23 July 2020; accepted: 21 November 2020

[1]Institute of Neural Tissue Engineering, Mudanjiang College of Medicine, Mudanjiang, China
[2]Department of Anatomy, School of Basic Medical Sciences, Ningxia Medical University, Yinchuan, China
[3]Center for Reproductive Biology and Health, College of Agricultural Sciences, The Pennsylvania State University, University Park, PA, USA
[4]Department of Otorhinolaryngology, The Second Affiliated Hospital, Mudanjiang College of Medicine, Mudanjiang, China
[5]Department of Pharmacology, Mudanjiang College of Medicine, Mudanjiang, China
[6]Department of Basic Psychological, Mudanjiang College of Medicine, Mudanjiang, China

†Equal contributors.

Corresponding authors:
Ying Wang, Institute of Neural Tissue Engineering, Professor of Anatomy, Mudanjiang College of Medicine, Tongxiang St, Aimin District, Mudanjiang, Heilongjiang 157011, China.
Email: yingwang2016@sina.com

Chun-Mei Li, Department of Basic Psychological, Mudanjiang College of Medicine, Tongxiang St, Aimin District, Mudanjiang, Heilongjiang 157011, China.
Email: pretty_926@163.com

Introduction

Peripheral nerve injury (PNI) is a global health concern, as neuromuscular targeting and recovery of function is often unsatisfactory for patients despite the regenerative capacity of peripheral nerves. The poor target reinnervation is primarily a result of too few regenerating axons, diminished trophic support and aberrant guidance of the axons that do regenerate.[1,2] Further complicating proper regeneration of peripheral axons is the degree of damage to the nerve and the need to repair or place a graft, often acellular nerve allografts (ANAs) to bridge a nerve gap in severe injuries. To aid in regeneration through ANAs, bone marrow stromal cell (BMSC) transplantation into the graft has been one promising approach to improve axonal regeneration and functional recovery. BMSCs exhibit many characteristics that are beneficial for transplantation including a rapid replication period and minimal immune response by the host tissue. In demonstration of other positive aspects of BMSCs in such therapy is the differentiation capacity toward Schwann cell lineage and the production and secretion of various neurotrophic factors.[3,4]

Of the neurotrophic factors, brain derived neurotrophic factor (BDNF) is one the most studied and therapeutically beneficial for axon regeneration in peripheral nerves. In the nerve, BDNF is produced and secreted by transformed Schwann cells, and imparts axon elongation through binding and activation of the tropomycin receptor kinase B (TrkB) on regenerating axons. In this regard, BDNF is a multifunctional neurotrophic factor that has both neuroprotective and regenerative influence on neurons and glial cells in the peripheral and central nervous systems. Local treatment with recombinant human BDNF (rhBDNF) on the repaired injured nerve enhances early regeneration in murine models of peripheral nerve injury.[5,6] However, some limitations persist concerning the general application and specific use of BDNF in promoting sciatic nerve injury repair and regeneration. Being a large molecule (13 kD), rhBDNF is not capable of effectively crossing the blood-brain or blood-nerve barrier.[7,8] The half-life of rhBDNF is relatively short, as well (a maximum of a few hours).[9,10] Experimental use of rhBDNF has previously been administered high doses,[11] which costly and increases potential risk of adverse side effects.[12–14] Such limitations led to identification of small molecules capable of mimicking the BDNF mechanism, but with improved selectivity and therapeutic control. As 7, 8-DHF is small and can cross the blood–brain/blood–nerve barrier in previously published experiments, the doses of 7, 8-DHF have been relatively low, and have exhibited no serious adverse side effects. Thus, 7, 8-DHF was appealing as an alternative to rhBDNF for enhancing axon regeneration in transected peripheral nerves.[15]

It has been shown that 7, 8-DHF is a powerful BDNF analog and TrkB agonist, inducing robust activation of TrkB in the mouse brain[16] and is neuroprotective under toxic neural environments involving oxidative and excitotoxic stress.[17] 7, 8-DHF activates the TrkB receptor, and upregulates the downstream extracellular signal-regulated kinase (ERK1/2) pathway in hippocampal neurons as well as primary rat retinal ganglion cells (RGCs).[18,19] Activation of Erk1/2 promote axon regeneration,[20] cells differentiation,[18] and survival,[21] and these effects were mostly blocked by application of a specific ERK inhibitor, U0126.

Previous studies have also demonstrated a neuroprotective effect from overexpressing BDNF in BMSCs-for treatment and repair of spinal cord injury and stroke.[22,23] For example, overexpressing BDNF enhances transplanted BMSC survival in a contused spinal cord, increases synaptic plasticity and neurogenesis via neuroprotective or/and angioprotective effects. Nevertheless, the influence and mechanism of 7, 8-DHF on BMSCs remain unclear. In light of these evidences, we hypothesize that 7, 8-DHF activates ERK1/2 signaling pathway via TrkB in BMSCs, subsequently promoting BMSCs proliferation, differentiation, and survival. Therefore, 7, 8-DHF therapy combined with transplantation of BMSCs in an ANA optimize axon regeneration, target musculature reinnervation, recovery of function following PNI (Figure 1). In the present study, we tested this combined treatment for repairing a sciatic nerve gap, to assess possible benefits to BMSC survival post-transplantation, axon regeneration, functional recovery, and possible mechanisms responsible for any documented therapeutic benefits.

Materials and methods

BMSC isolation and culture

In preparation of BMSCs for use in the study, BMSCs were obtained from adult female mice and cultured in standard culture medium consisting of Dulbecco's modified Eagle's medium (DMEM) with 10% fetal bovine serum (FBS, ThermoFisher Scientific, Pittsburgh, PA, USA) as described previously.[3] In brief, bone marrow was removed from the marrow cavity of dissected mouse long bones and the isolated cells were centrifuged in culture medium. The supernatant was removed and cells in the pellet were re-suspended in standard culture medium and cultured in a humidified 37°C incubator containing 5% CO_2 for 48 h. Cells that did not adhere to the culture dish were removed. Next, fresh medium was replaced every 3 days in the adherent cells, and the cells at this stage were labeled passage 0 (P0). To expand the isolated cell culture, once the cells achieved 85% confluence, the cells were detached from the culture dish using trypsin and split to new culture plates. This process was repeated two to three more times, and passage 4 BMSCs seeded in culture plates were used in all associated experiments in the study.

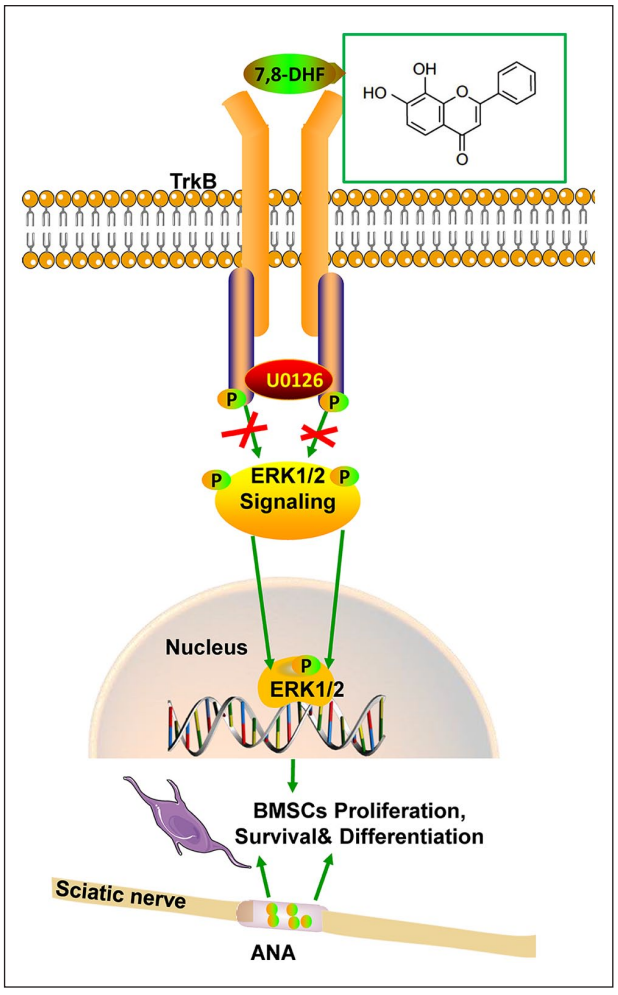

Figure 1. Schematic overview of 7, 8-DHF induced TrkB signaling cascade in BMSCs in ANA. 7, 8 DHF acts on the TrkB receptor, the activation of TrkB stimulates downstream proliferation, differentiation and survival signaling molecules ERK1/2 in transplanted BMSCs in ANA.

To identify and confirm the status of the cultured BMSCs, the cells were fixed with 4% (wt/vol) paraformaldehyde (PFA) 30 min at room temperature (RT), blocked for non-specific binding and immunolabeled with anti-CD29 (Armenian hamster monoclonal; 1:200) anti-CD90 (human monoclonal; 1:200), anti-CD45 (rat monoclonal; 1:200) and anti-CD34 antibodies rat Monoclonal; 1:200; ThermoFisher) overnight at 4°C. The next day, appropriate FITC-conjugated secondary antibodies (1:200; goat polyclonal; Sigma-Aldrich, St. Louis, MO, USA) were incubated with the primary antibody-labeled cells for 1 h at RT, followed by labeling of nuclei with DAPI (1:200; Sigma). The labeled slides were then imaged using an Olympus BX41 epifluorescent microscope. Cells treated with phosphate-buffered saline (PBS) only (0.01 M, pH 7.4) was the experimental negative control, and the ratio of FITC+ cells to all DAPI-labeled cells was calculated to determine purity of BMSCs.

Treatment of BMSC with 7, 8-DHF

The compound 7, 8-DHF was purchased from Sigma (⩾98%). 7, 8-DHF was dissolved in PBS with 17% dimethyl sulfoxide (DMSO). BMSCs were seeded into 6-well culture plates at a density of (2×10^7 cells/well) and cultured to ~90% confluence. BMSCs were treated with 7, 8-DHF using an optimal concentration of 500 nMol/L, as determined in a previous study, for 72 h.[24] Fresh culture medium was replaced, and the BMSCs were separated into four experimental groups: (1) a negative control (NC) group, treated with medium only, (2) cells treated with 7, 8-DHF, (3) 7, 8-DHF + U0126 group, the cells were treated with 7, 8-DHF and U0126 (selective inhibitor of ERK1/2 signaling, 5 µM, Sigma-Aldrich, St. Louis, MO, USA), and (4) BDNF group, the cells were treated with human recombinant BDNF (159 nMol/L, Sigma).[18] Following the treatment period, protein was isolated from the BMSCs for ELISA and Western blot analysis.

ELISA analysis

ELISA was performed as described in prior studies.[21] In brief, the supernatant from the conditioned medium all groups of cells were collected and quickly frozen at −80°C. The ELISA kit (R&D Systems, Minneapolis, MN) was used to determine the amount of BDNF protein according to the manufacturer's protocol. The above experiments were repeated three times.

Western blot

Protein analysis was performed via Western blot as described previously.[25] In brief, for our in vitro experiments, each BMSC sample was collected and homogenized after 3 days in the four groups. To assess protein expression in vivo, ANAs were isolated from the different groups and rapidly frozen on dry ice 4 weeks following engraftment. Protein samples (20 µg) were loaded into 10% SDS-polyacrylamide gels for electrophoresis and transferred to polyvinylidene difluoride (PVDF) membranes (Millipore, Bedford, MA, USA). After transfer, the membrane was blocked for non-specific labeling with 5% skim milk powder for 1 h at RT. We incubated the membranes at 4°C overnight with antibodies targeting TrkB (rabbit polyclonal; 1:500), phospho-ERK1/2$^{Thr202,\ Tyr204}$ (mouse monoclonal; 1:1000), total-ERK1/2 (rabbit polyclonal; 1:1000), and glyceraldehyde 3-phosphate dehydrogenase (GAPDH) (rabbit polyclonal; 1:500; ThermoFisher) as a loading control. Following primary antibody labeling, membranes were incubated with a secondary antibody conjugated with horseradish peroxidase (HRP) for 1 h at RT (goat anti-rabbit or mouse polyclonal; 1:3000; ThermoFisher). An enhanced chemiluminescence (ECL) kit (GE Healthcare, Little Chalfont, UK) and a Gel Doc EQ System with Universal Hood II imaging system

(Bio-Rad, Hercules, CA, USA) were used to observe and image positive labeling. The membrane images were then analyzed using the accompanying Gel Doc software.

BMSC proliferation assay

To determine whether 7, 8-DHF influenced the proliferation of BMSCs, four BMSC groups were seeded (1.25×10^3 cells/well) in 96-well plates with fresh culture medium for varying periods of time (1, 2, 4, 6, and 8 days). The culture medium was changed daily. At each time point, we assessed BMSC proliferation/viability using a 3-[4, 5-dimethylthiazol-2-yl]-2, 5-diphenyl tetrazolium bromide (MTT) assay (Promega, Madison, WI, USA) according to the manufacturer's protocol. We added 10 µl of a MTT solution (12 mM) into each well and incubated the cells for 4 h at 37°C. The absorbance in each well was then read at 570 nm using a microplate reader (Thermo, USA). The experiment was repeated in triplicate.

Starvation effects on BMSC viability

For determining BMSC viability response to nutrient deprivation, the cells were plated in 96-well plates (1.25×10^6 cells/well) with DMEM only (no serum) and cultured for 1, 2, 4, 6, or 8 days.[33] The medium was replaced daily, and viability of the cells was evaluated with an MTT assay at the stated time points. All experimental concentrations were assessed in triplicate.

Differentiation of BMSCs into Schwann cell-like cells and flow cytometry analysis

To evaluate the effects of 7, 8-DHF on BMSC differentiation, BMSCs were incubated in serum-free DMEM containing 1 mM β-mercaptoethanol (β-ME) (Sigma-Aldrich, USA) for 24 h. Then the culture medium was replaced with DMEM + 10% FBS and 35 ng/ml all trans-retinoic acid (RA) (Sigma-Aldrich) to stimulate differentiation. Three days later, the induction medium that consisted of DMEM, 10% FBS, 5 µM forskolin (Sigma), 200 ng/ml recombinant human heregulin-β1 (HRG) (PeproTech), 10 ng/ml basic fibroblast growth factor (bFGF) (R&D Systems), and 5 ng/ml recombinant rat platelet-derived growth factor (PDGF)-AB (R&D Systems) were added for 10 days.[21] Differentiated cells were digested by trypsinization (0.25% trypsin) and fixed with 4% paraformaldehyde (PFA), then were immunolabeled with primary antibody against S-100 (1:200; Sigma Aldrich) and DAPI (1:200; Sigma Aldrich). Then cells were incubated with a fluorescent goat anti-rabbit IgG (FITC) (1:200; Sigma Aldrich). The ratio of S100+ cells was analyzed using an Olympus BX41 epifluorescent microscope. An investigated blinded to the treatment conditions performed all analysis.

Labeling of the differentiated BMSCs with the Schwann cell marker, S100 was analyzed by flow cytometry. Cells were labeled using an antibody against S100 (1:500; Sigma Aldrich), and BMSC expression of S100 was assessed by using flow cytometer (BD Bioscience).[26]

Animals

A total of 60 C57BL6 mice (half males and half females) weighing ~22 g and 24 adult female CD1 (ICR) mice were acquired from the Experimental Animal Center of China Medical University (Shenyang, China; Certification No. SCXK Liao 2013-0001). Animals were provided ad libitum access to water and food and housed four mice/cage maximum. The ICR mice were used as nerve tissue and BMSC donors, and C57BL6 mice received the grafts. All experiments involving the use of animals were approved by the Animal Care and Use Committee of China Medical University.

Preparation of ANAs

Preparation of the acellular nerve allografts (ANA) was achieved as described previously.[27] In brief, we anesthetized 24 CD1 (ICR) mice and harvested 10 mm sciatic nerve segments bilaterally spanning from the lumbosacral nerve region to terminal branches. The severed ends of the 48 harvested nerves were fixed followed by incubation at 4°C with 0.05 M Tris-HCl buffer plus protease inhibitors (aprotinin, 0.1 µg/ml; leupeptin, 0.5 µg/ml; pepstatin A, 0.6 g/ml) for four days. Following this incubation period, DNase I and RNase A (5 ng/ml and 1 U/ml, respectively) were mixed in Tris-HCl buffer+3% Triton X-100 (pH 7.4) for nerve digestion. Digestion lasted 10 h.

PKH26, a fluorescent tracking dye, was applied to BMSC cultures before their engraftment in accordance with the included instructions (Sigma). The ANA treatment groups were designated as follows: (1) a control group with the ANA injected with DMEM only, (2) bilateral microinjections of 7, 8-DHF (500 nMol/side) into the ANA.[24] A total 5 µl was injected slowly into each side over a 1-min period, and the needle placement was maintained for one additional minute. Following injection, ANA transplantation was performed, (3) engraftment of the ANA with BMSCs; A Hamilton syringe with a 30-gauge needle and a microinjector was used to inject 1×10^7 BMSCs in 5 µl medium at four sites spaced evenly along the ANA. Next, the ANAs were placed in culture and incubated in a 5% CO_2 incubator at 37°C for 48 h, and (4) BMSCs +7, 8 DHF treatment of the ANAs. To perform additional ultrastructural analysis, we collected in vitro ANAs or those following 24 h surgery in vivo and fixed them in 2.5% glutaraldehyde, post-fixed in 4% (wt/vol) osmium tetroxide (Sigma), followed by dehydration via a graded ethanol

series. Then, the ANAs were dried using a critical point drier, followed by gold-coating for electron microscopy. ANA cross sections were prepared and imaged using a scanning electron microscopy (SEM, JSM-T300, Jeol Ltd., Tokyo, Japan).

Experimental groups and surgical procedures

All mice were randomly assigned to five groups (12 mice/group): Group I: ANA + DMEM; Group II: ANA+7, 8 DHF; Group III: ANA+BMSCs; Group IV: ANA+BMSCs+7, 8-DHF, and Group V: Autograft, autologous nerve bridging. Creation of a sciatic nerve gap defect and ANA engraftment was performed as previously described. In brief, the dorsal surface of the hindlimbs was shaved using electric clippers, followed by disinfection of the skin with betadine solution and 70% alcohol wipes prior to surgery. To anesthetize the mice, the animals received intraperitoneal (i.p.) injection of 10 g/L chloral hydrate (100 mg/kg) and the right sciatic nerve was surgically exposed. The sciatic nerve was transected twice at a distance of 10 mm between each cut, and the 10-mm nerve segment was removed to create a nerve gap. The resulting nerve gap was bridged in all five experimental groups of mice using one of the described ANA engraftment paradigms. The nerve gap was repaired with reversed sciatic nerve segments taken from nerves from the operative side. The ANA was transplanted to bridge the nerve gap using 9/0 nylon suture to connect the ANA to the proximal and distal nerve stumps. Then, the muscles and skin were closed, and mice were placed in a home cage on a heating pad maintained at 37°C until complete recovery from anesthesia. At 1, 24, 48, and 72 h post- surgery, the animals received 7, 8-DHF injections (5 mg/kg) (Groups II and IV) according to previously described methods.[28]

HRP retrograde neural tracing

Retrograde tracing was accomplished using HRP-conjugated cholera toxin B subunit (BHRP). This was performed to label lumbar spinal cord motor neurons according to previously established methods.[29] In brief, 26 days after surgery, all animals were anesthetized again and the tibialis anterior (TA) muscles were exposed. BHRP (2 µl, 0.2%; List Biological, Inc., Campbell, CA, USA) was injected with a Hamilton microsyringe and a 25-gauge needle across three regions within each muscle. The needle and microsyringe was connected by polyethylene tubing. BHRP was slowly administered to the muscle tissue using a mechanical Microdrive. The syringe and needle were left in place for a minimum of 2 min to prevent leakage of tracer from the injection site. Using this technique, L3-L5 ipsilateral motor neurons were labeled revealing detailed neuronal morphology and their dendrite arbors. Forty-eight hours following BHRP injection, the animals were euthanized with Nembutal (60 mg/kg, i.p.) followed by cardial perfusion with saline and an ice-cold fixative solution containing 1% paraformaldehyde/1.25% glutaraldehyde. The labeled cells were counted in each tissue section and the total per animal was calculated. A section not incubated BHRP was used as a negative control. All described analyses were performed by a blinded investigator with no knowledge of the treatments or groups.

Immunofluorescence and immunohistochemistry

Immunolabeling of cells and tissue sections was performed based on our previously described methods.[3,25] Briefly, the harvested grafted nerve was serially cryosectioned longitudinally or transversely at 25 µm thickness, followed by mounting on onto Superfrost Plus slides (ThermoFisher). The mounted tissues were incubated with antibodies targeting S100 (rabbit polyclonal; 1:200; Sigma) for labelling Schwann cell-myelinated fibers, and neurofilament (NF, rabbit polyclonal; 1:200; Sigma) for axonal labeling. Next, the tissues were incubated with FITC-conjugated secondary antibody (1:200; goat anti-rabbit Polyclonal; Sigma) or AlexaFluor 555-conjungated secondary antibody (1:200; donkey anti-rabbit polyclonal; ThermoFisher) and imaged via epifluorescent microscopy.

The L4-5 spinal cord was dissected and harvested from the mice, and 25 µm thick serial cross-sections were obtained using a cryostat and mounted on microscope slides. The mounted sections were treated with 3% hydrogen peroxide solution for 10 min at room temperature to quench endogenous peroxidase, followed by three 10 min PBS washes. The sections were then blocked for non-specific labeling using 5% bovine serum albumin (Sigma) in PBS for 30 min at 37°C. The sections were then incubated overnight at 4°C with rabbit polyclonal anti-BDNF (1:200; Abcam, Cambridge, MA, USA), and TrkB (rabbit polyclonal; 1:200; ThermoFisher). Next, the sections were incubated for one additional hour with biotin-conjugated secondary antibody. Secondary antibody signal was increased using a Vector Elite ABC kit (ThermoFisher) and visualized using 0.02% 3,3′-diaminobenzidine (DAB; ThermoFisher).

For negative controls, sections were treated with PBS only with all other steps the same as described above. MetaMorph software (Molecular Devices, Inc., San Jose, CA, USA) was utilized for image acquisition of the tissue and integrated optical density (IOD) analysis of the fluorescent signal of positive immunolabeling or the number of positive cells. These analyses were performed by a researcher blinded to all treatment conditions.

Histologic analysis

The regeneration of injured nerve was assessed using prior published histological methods.[27,30] Briefly, samples harvested from the center of the regenerating ANAs were

fixed overnight in a solution of 2% glutaraldehyde and 5% sucrose in 0.1 M sodium cacodylate buffer (pH 7.4). The next day, the tissues were incubated for 1 h with 4% osmium tetroxide solution. Spurr's epoxy resin was used to embed the tissue, and the resin-embedded tissue was cured at 70°C. Once cured, the samples were cut into 1 µm semi-thin sections. In addition, 70 nm ultra-thin sections were also prepared. Toluidine Blue O (1% in sodium borate; Sigma) was used to stain semi-thin sections and 10 random fields were imaged per section from each group to evaluate myelinated axons, myelin sheath thickness, and diameter of axons using Stereo Investigator software (MicroBrightField, Inc., Williston, VT, USA). Ultra-thin sections were gathered on copper mesh grids (600 bars/in) and counterstained with 4% uranyl acetate in 50% ethanol and Reynolds' lead citrate. The ultra-thin cross sections were finally imaged and examined using a Hitachi H600 electron microscope (accelerating voltage = 80 kV). The G-ratio (the inner diameter of the axon/the outer diameter of the entire fiber) was calculated using Image J to evaluate the myelination of regenerating axons. At least 100 myelinated axons were randomly selected for calculation in each animal.

Skeletal muscle motor endplate analysis

A muscle tissue was isolated from middle of the TA muscle belly 28 days following engraftment, and motor endplate densities were analyzed after acetylcholinesterase labeling using the Roots-Karnovsky method, as described previously.[31] Briefly, isolated TA muscles were placed in fixative overnight, followed by transfer 10% w/v sucrose phosphate buffer (pH 7.4) for cryoprotection. Next, the muscles were washed in distilled water and flash frozen in 2-methylbutane on dry ice. Muscle tissues were longitudinally sectioned using a cryostat and thaw mounted onto SuperFrost glass slides. Acetylcholinesterase labeling of motor endplates allowed calculation of their density using the Roots-Karnovsky method. Thirty-five muscle fibers and 30 endplates per animal were quantified on average at 500× magnification. Motor endplate number per muscle fiber was estimated by quantifying muscle fibers and endplates in a 1 mm × 1 mm grid from a randomly selected muscle section region (1 sample field/section, 5 sections/animal). On average, 150 muscle fibers per animal were assessed. Fiber and endplate areas were averaged for each animal for further analysis.

Electrophysiological assessment of neuromuscular function

To evaluate neuromuscular function post-sciatic nerve graft, electrophysiological analysis was performed on all animals on day 42 prior to euthanasia. For this procedure, all mice were anesthetized with pentobarbital (40 mg/kg i.p.) and the sciatic nerve was surgically exposed. The sciatic nerve was then stimulated at the sciatic notch by two needle electrodes and stimulations of 0.05 ms until above maximal intensity was reached. Physiological responses were defined by amplitudes greater than 0.15 mV and latencies less than 25 ms. Small needle electrodes were positioned in the plantar and medial gastrocnemius muscles to record compound action potentials (CAPs) after sciatic nerve stimulation. To visualize evoked action potentials, an oscilloscope (Sapphire 4M, Medelec Vickers) was utilized, and amplitude measurements from baseline to peak and latency to onset were calculated. Then, compound action potential amplitude (CAMP) and latency period were recorded.[32]

Sciatic function index (SFI) assessment

The sciatic function index (SFI) was used to assess hindlimb functional ability in sciatic nerve engrafted mice.[33] SFI assessment was performed weekly after surgery by researchers blinded to animal treatment information. Mice hindpaws were colored with ink, and the animals were allowed to walk freely through a plastic tunnel with paper covering the walkway. Pawprints on the paper were analyzed, and the distances between the heel and third toe (PL), first and fifth toes (TS), and second and fourth toes (ITS) of the hindpaw on surgery side (EPL, ETS, and EITS, respectively) and the unaffected contralateral side (NPL, NTS, and NITS, respectively) were calculated. The following formula was used to calculate SFI: $SFI = -38.3 \times (EPL-NPL)/NPL + 109.5 \times (ETS-NTS)/NTS + 13.3 \times (EITS-NITS)/NITS - 8.8$.

Statistical analysis

SPSS software (ver. 13.0; SPSS, IL, USA) was used for all statistical analyses. All values were expressed as mean ± standard deviation (SD). Determination of sample sizes was accomplished through calculating the minimum animal or assessment number required for adequate statistical power analysis. All experimental groups in the study included more than the minimal number of animals indicated by the power analysis. For comparison of data between three or more groups, a one-way ANOVA with Tukey's post-hoc test was performed. A p value <0.05 was considered statistically significant.

Results

BMSC morphology and phenotype

From passages ranging from 1 to 4, cell morphology was consistent with that of BMSCs as observed with a microscope (Figure 2(a)). For BMSC identification confirmation, the cells were labeled with either CD29, CD90, CD34, or CD45 antibodies, and DAPI was used to label cell nuclei. Cells confirmed as BMSCs presented double-labeling with

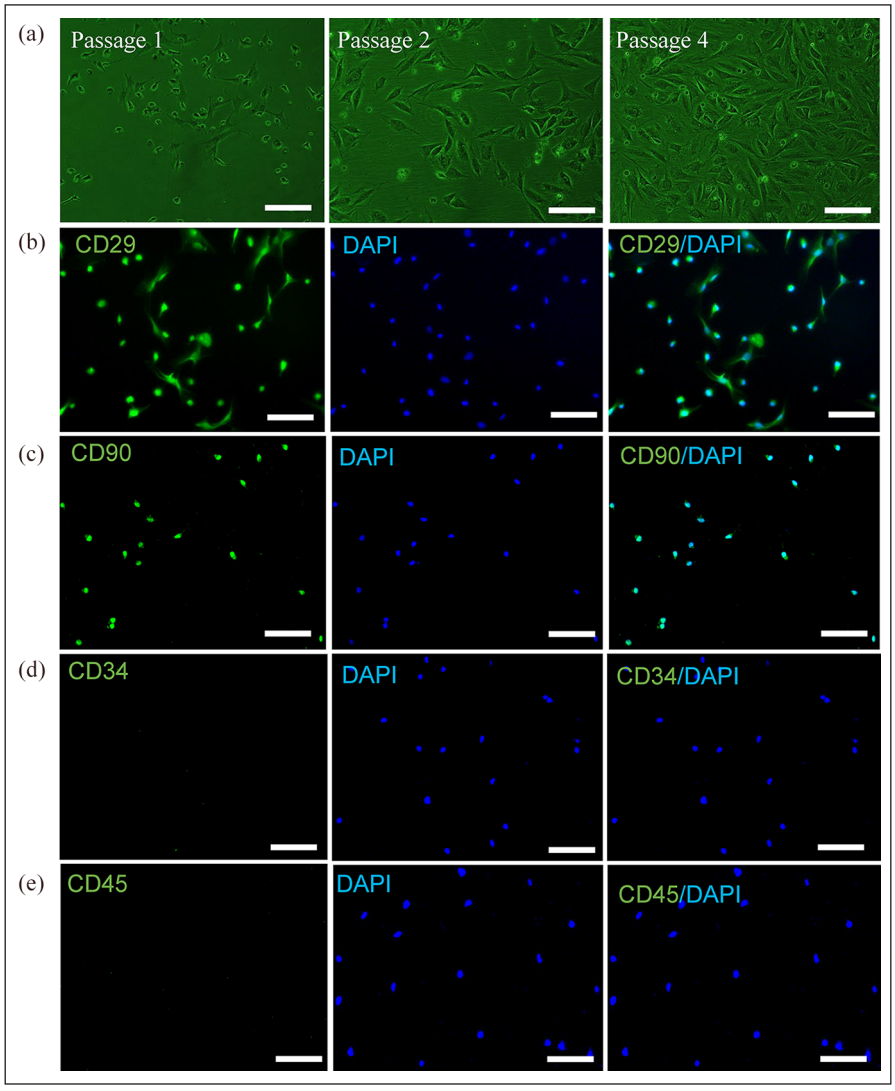

Figure 2. Characterization of BMSC morphology and phenotype. (a) BMSCs at passage 1, 2, and 4. (b–e) Immunohistochemical labeling of BMSCs by antibodies against CD29, CD90, CD34, or CD45 (green) with nuclear co-labeling (DAPI; blue). The merged image indicates that BMSCs were double labeled with CD29, CD90, CD34, or CD45 and DAPI. Scale bars = 100 μm.

DAPI and cytoplasmic MSC markers CD29 (97.5%) and CD90 (98.2%) (Figure 2(b) and (c)). BMSCs showed no labeling by hematopoietic stem cell markers CD34 (0.2%) or CD45 (0.0%) (Figure 2(d) and (e)).

7, 8-DHF stimulated BMSC TrkB expression and Erk phosphorylation in vitro

Compared to the NC group, TrkB expression was significantly increased in the 7, 8-DHF, 7, 8-DHF +U0126 and BDNF groups ($F_{3,\ 8}=74.45$, $p<0.001$), however, no significant difference in TrkB expression was observed among cells in the 7, 8-DHF group, 7, 8-DHF +U0126 group and BDNF group (Figure 3(a) and (b)). In addition, the ratios of p-ERK1/2/t-ERK1/2 expression were elevated in the 7, 8-DHF group and BDNF group compared to the NC group, however, the upregulation of the p-ERK1/2/t-ERK1/2 expression was significantly inhibited by U0126 ($F_{3,\ 8}=18.51$, $p<0.001$) (Figure 3(a) and (c)). Furthermore, we found that secreted BDNF levels were significantly increased in the BDNF group compared with other three groups, and no significant differences in BDNF expression among NC, 7, 8-DHF, and 7, 8-DHF +U0126 group ($F_{3,\ 8}=35.77$, $p<0.001$) (Figure 3(d)). Our results indicate 7, 8-DHF upregulated TrkB expression and enhanced downstream Erk phosphorylation similar to the BDNF group, and 7, 8 -DHF activates the Erk phosphorylation was almost completely blocked by application of U0126.

7, 8-DHF promoted BMSCs proliferation and survival in vitro

We assessed cell proliferation using a 3-(4, 5-dimethylthiazolyl-2)-2, 5-diphenyltetrazolium bromide (MTT) assay.

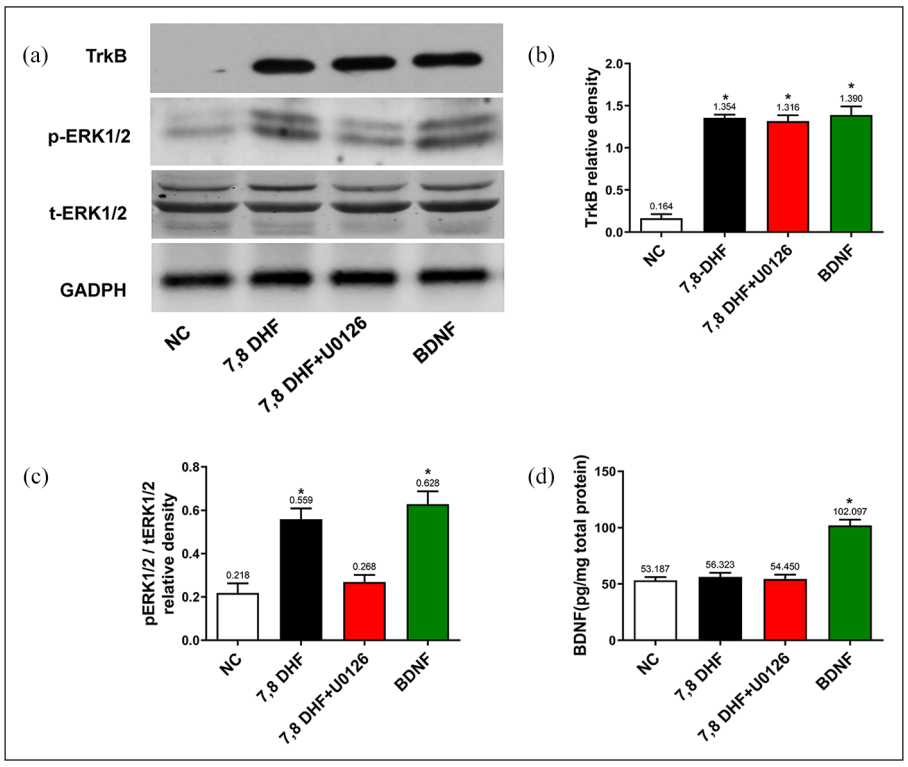

Figure 3. 7, 8-DHF stimulates TrkB and the downstream Erk phosphorylation. (a) Representative Western blots of TrkB expression and p-ERK1/2 to t-ERK1/2 expression ratios in four groups of cultured BMSCs shown at 3 days in vitro ($n = 4$). Graphs from the respective analyses represent the relative density of labeling as a measure of expression for these markers (b, c). ELISA analysis determined BDNF levels secreted from the four groups of BMSCs at 3 days in vitro ($n = 3$) (d). Error bars = SD. *$p < 0.05$, versus NC group. Data were analyzed with a one-way ANOVA followed by Tukey's post hoc test.

BMSC proliferation was significantly increased at day 8 in the 7, 8-DHF group and BDNF group compared with the NC group and 7, 8-DHF +U0126 group ($F_{3,\ 8} = 12.97$, $p < 0.001$) (Figure 4(a)).

To determine the effects of 7, 8-DHF on the survival of BMSCs, BMSCs in the BDNF, 7, 8-DHF and NC groups were nutrient-deprived by culture in DMEM without serum. An MTT assay also indicated that BMSC survival was significantly higher in the 7, 8-DHF group and BDNF group compared to the NC group and 7, 8-DHF +U0126 group at days 2, 4, 6, and 8 (2 days: $F_{3,\ 8} = 12.63$, $p < 0.01$; 4 days: $F_{3,\ 8} = 29.74$, $p < 0.001$; 6 days: $F_{3,\ 8} = 7.837$, $p < 0.01$; 8 days: $F_{3,\ 8} = 9.942$, $p < 0.01$) (Figure 4(b)).

The observed results indicate that treatment with 7, 8-DHF promotes BMSC proliferation and survival, and mimics the effect of BDNF treatment. These effect of 7, 8-DHF was mostly blocked by application of U0126.

7, 8-DHF improved Schwann-like cell differentiation of BMSCs

Ten days following induction, the BDNF group, 7, 8-DHF group and 7, 8-DHF +U0126 group exhibited a greater ratio of S100+ cells than the NC group. Moreover, the ratio of S100+ cells in the 7, 8-DHF group was greater in comparison to the 7, 8-DHF +U0126 group, no significant differences in the ratio of $S100^+$ cells between the 7, 8-DHF and BDNF groups ($F_{3,\ 12} = 39.95$, $p < 0.001$) (Figure 4(c) and ((d)). The number of surviving cells was also elevated in the BDNF group, 7, 8-DHF group and 7, 8-DHF +U0126 group compared to the NC group, and the number of surviving cells in the 7, 8-DHF group was greater in comparison to the 7, 8-DHF +U0126 group, no significant differences in surviving cells between the 7, 8-DHF and BDNF groups ($F_{3,\ 12} = 34.00$, $p < 0.001$) (Figure 4(c) and (e)). Furthermore, flow cytometry showed that the proportions of S100 labeling in the NC, 7, 8-DHF, 7, 8-DHF +U0126 and BDNF groups were 26.77%, 45.84%, 34.88%, and 48.69%, respectively (Figure 4(f)).

These findings indicate that 7, 8-DHF enhances survival and Schwann-like cell differentiation of BMSCs, and the results were comparable to that of the BDNF group, which was partially blocked by application of U0126.

Structure of 7, 8-DHF +BMSCs-ANA and bridge ANA to the nerve gap

To evaluate the contents of the ANA at the ultrastructural level, SEM images of the ANA cross-sections showed that axons and myelin sheaths were deficient, while the

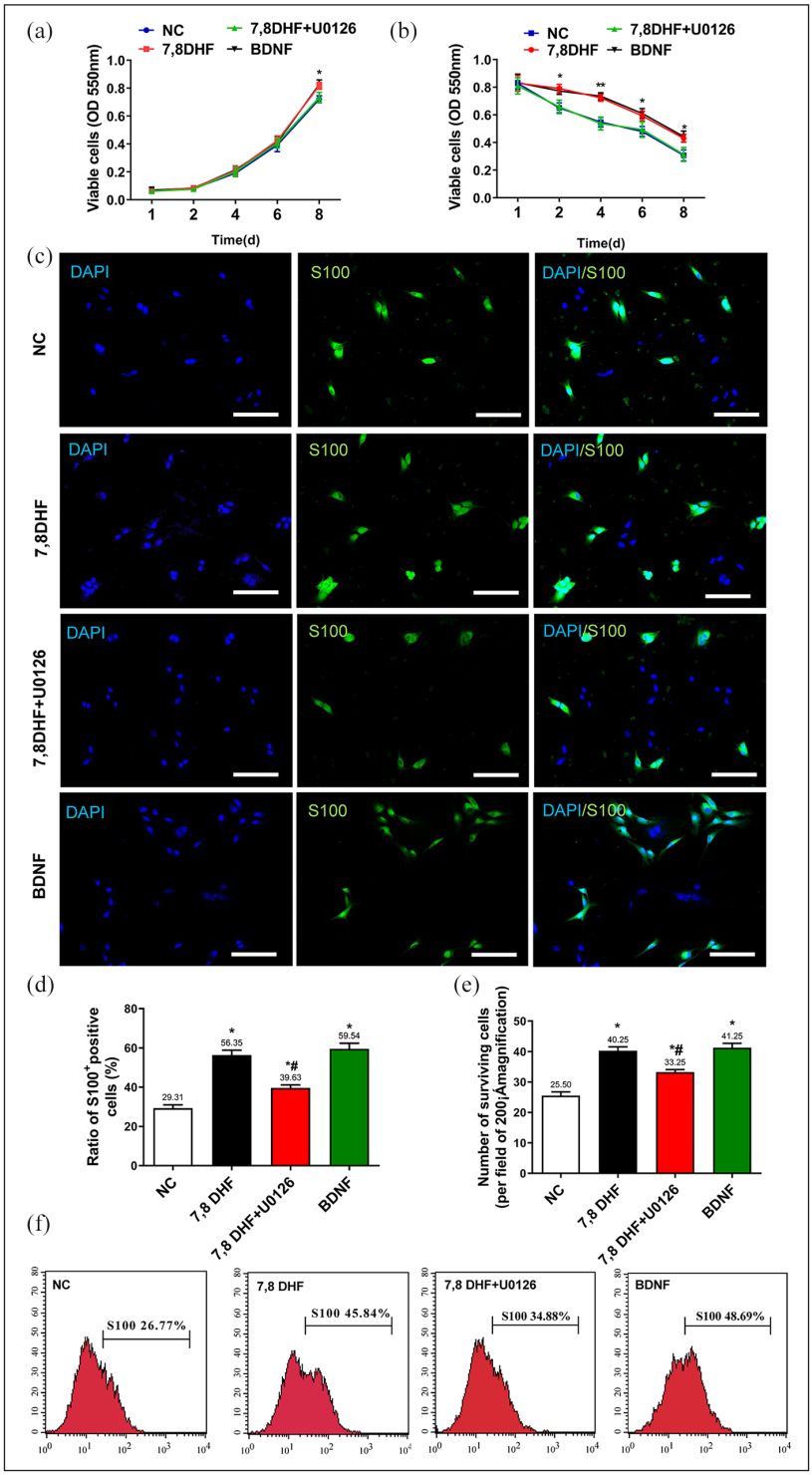

Figure 4. 7, 8-DHF enhances BMSC proliferation, survival and Schwann-like cell differentiation. (a) Four BMSC groups were incubated for 1, 2, 4, 6, or 8 days at 37°C and 5% CO_2. An MTT assay was used to assess cell proliferation. (b) Four BMSC groups were incubated with DMEM lacking serum for 1, 2, 4, 6, or 8 days. An MTT test was used to assess cell viability. The experiment was repeated three times. (c) Immunofluorescence images show S100+ cells labeled in green, and cell nuclei labeled in blue. Graphs represent that quantification and analysis of the ratio of S100+ cells (d) and the number of surviving cells (e). ($n = 4$). Scale bars = 100 μm. Error bars = SD. *$p < 0.05$, **$p < 0.01$, versus NC group, #$p < 0.05$ versus 7, 8-DHF group. The data were analyzed with a one-way ANOVA followed by Tukey's post hoc test. (f) Flow cytometry showed that the proportions of SCs markers S100 in four BMSC groups.

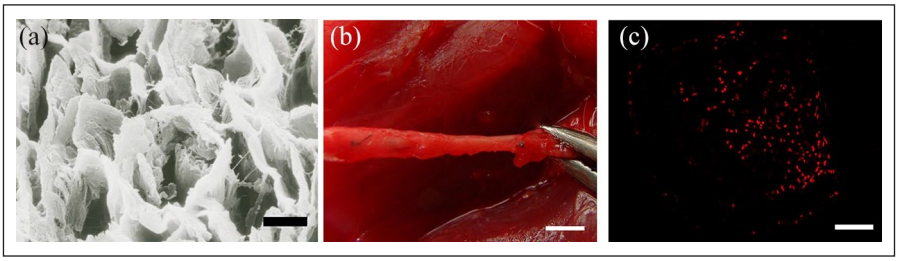

Figure 5. Structure of 7, 8-DHF+BMSCs-ANA and an ANA bridge only to repair a nerve gap. (a) Scanning electron micrographs (SEM) of the ANA cross sections. (b) ANAs were stitched to bridge both stumps of the sciatic nerve gap with 9-0 nylon sutures. (c) Fluorescence microscope observation of the cross sections showed that PKH26 labeled BMSCs (red) in the middle of ANA 24 h after surgery. Scale bar = 10 μm (a), 2 mm (b), 100 μm (c).

well-ordered endoneurial tubes stayed intact (Figure 5(a)). The nerve defect was bridged with a surgical engraftment of an ANA (Figure 5(b)), and 24 h post-surgery, fluorescence microscopy of nerve cross-sections indicated abundant red PKH26-labeled BMSCs within the ANA (Figure 5(c)).

7, 8-DHF promoted myelinated axon regeneration and transplanted BMSCs survival in regenerating ANAs

To evaluate axon regeneration, myelination, and survival of transplanted BMSCs in the regenerating ANA, longitudinal ANA sections were analyzed microscopically via immunohistochemical labeling (Figure 6(a)). BMSCs observed within the ANA in the ANA+BMSCs+7, 8-DHF treatment exhibited significantly elevated PKH26+ labeling in comparison to the ANA+BMSCs group; however, no PKH26+ BMSC labeling was detected in the ANA or ANA+7, 8-DHF groups ($F_{3,\ 20}=51.37$, $p<0.001$) (Figure 6(b)).

In assessment of whether transplanted BMSCs could differentiate into Schwann-like cells in vivo, we evaluated the extent of differentiated cells as indicated by double labeling between PKH26 and S-100 in the ANA+BMSCs +7, 8-DHF groups. This co-localization was minimal in both the ANA+BMSCs and ANA+BMSCs+7, 8-DHF groups. These findings confirm that the differentiation of BMSC into Schwann-like cells was not influenced by 7, 8-DHF within the nerve grafts.

Intensity quantification of S-100 labeling revealed that significantly increased levels of peripheral myelin was observed in the ANA+BMSCs+7, 8-DHF and ANA+ BMSCs groups compared to the ANA and ANA+7, 8-DHF groups. Furthermore, S-100 labeling was significantly elevated in the ANA+BMSCs+7, 8-DHF group in comparison to the ANA+BMSCs group. No difference in expression was observed in the ANA and ANA+7, 8-DHF groups ($F_{3,\ 20}=49.52$, $p<0.001$) (Figure 6(c)). Our results indicate that 7, 8-DHF+BMSCs treatment improves BMSC survival and promotes regeneration of myelinated axons in ANAs.

7, 8-DHF+BMSCs enhanced myelinated fiber and axon regeneration in regenerating ANAs

To assess the number and myelination quality of axons within the ANAs, toluidine blue staining and TEM was performed. These techniques demonstrated that the number of myelinated axons, myelin thickness, axon diameter and G-ratio in the ANA+BMSCs and ANA+BMSCs+7, 8-DHF groups were increased in comparison to the ANA and ANA+7, 8-DHF groups. The number of myelinated axons, axon diameter, and G-ratio calculated in the ANA+BMSCs+7, 8-DHF group was significantly greater compared to the ANA+BMSCs group; however, there was no clear difference in myelinated axon number, myelin thickness, axon diameter or G-ratio between the ANA+BMSCs+7, 8-DHF group and the autograft group. Also, no differences were apparent between the ANA and ANA+7, 8-DHF groups, though a trend of increase was observed in the ANA+7, 8-DHF group (myelinated fiber number: $F_{4,\ 35}=29.29$, $p<0.0001$; thickness of myelin sheath: $F_{4,\ 35}=39.05$, $p<0.0001$; axon diameter: $F_{4,\ 35}=66.95$, $p<0.0001$; G-ratio: $F_{4,\ 35}=35.95$, $p<0.0001$) (Figure 7(a)–(e)).

Peripheral axon regeneration into the ANAs was analyzed by quantifying the number of neurofilament+ (NF+) axons present in transverse sections in the middle of ANA. We found that NF+ labeling within in the middle of the ANA exhibited a similar pattern of change under different treatment conditions ($F_{4,\ 35}=29.24$, $p<0.001$) (Figure 7(a) and (f)). The results revealed that 7, 8-DHF+BMSCs enhanced fiber myelination and axon regeneration into regenerating ANAs.

7, 8-DHF+BMSCs enhance the number of target muscle motor endplate

To determine whether 7, 8-DHF+BMSC treatment of ANA could promote TA muscle motor function recovery, motor endplate density in the TA muscle was analyzed post-injury (Figure 7(a)). Motor endplate number was increased in the ANA+BMSCs and ANA+BMSCs+7, 8-DHF groups compared to the ANA and ANA+7, 8 DHF

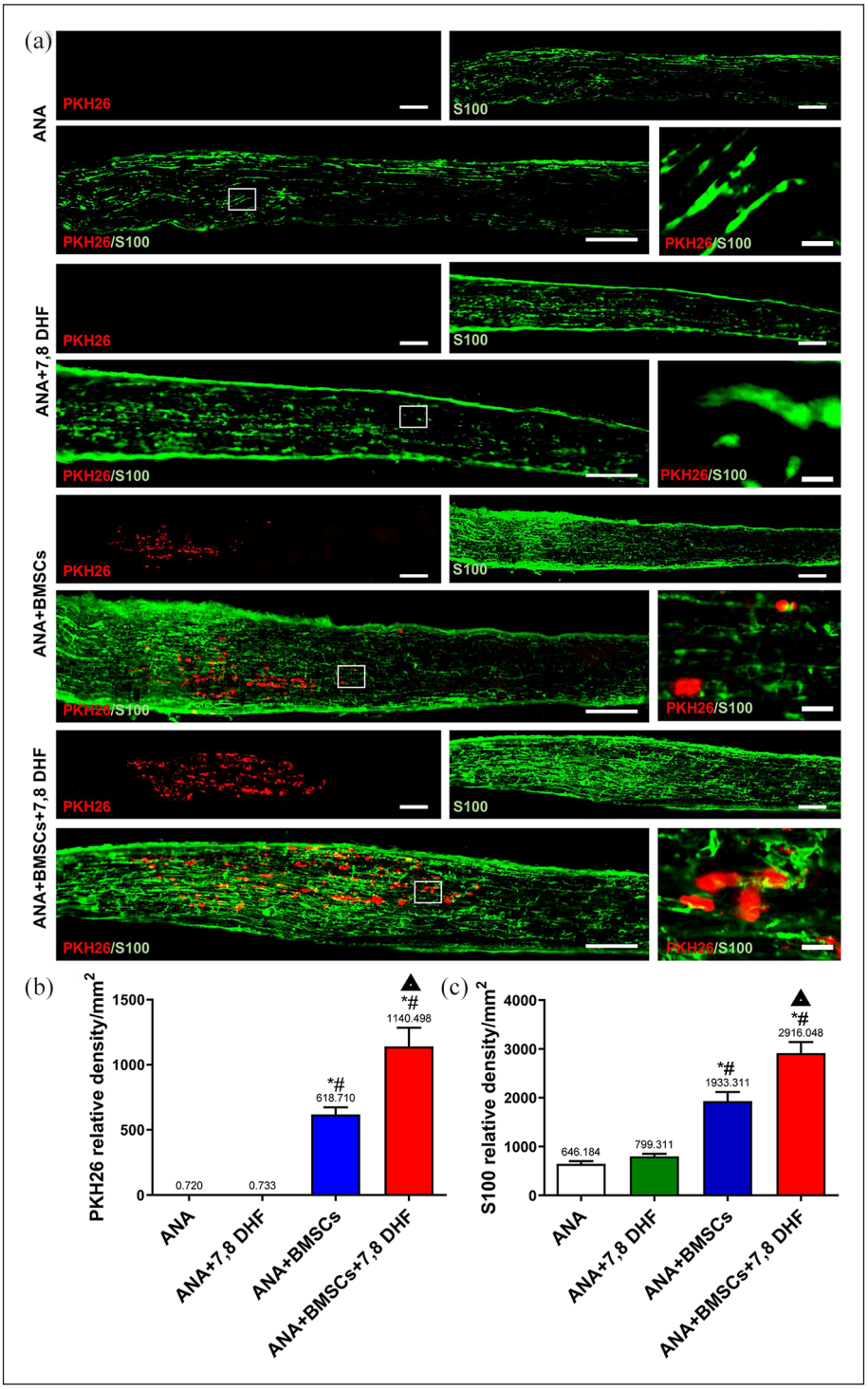

Figure 6. 7, 8-DHF+BMSCs significantly increased S-100 (myelinated fiber) expression and survival of transplanted BMSCs using PKH26 labeling in regenerating ANAs.

Representative immunofluorescence images of S-100 labeling (green) and a red fluorescent tracking dye, PKH26, labeling BMSCs in longitudinal ANA cryosections sections from all four ANA transplant groups 28 days post-surgery, the high magnification inserts of boxed area of interest shows that red labelled BMSCs do not co-localize much with green S100 staining ($n = 6$ mice/group) (a). Number of PKH26+ cells (b), S-100 protein expression and (c) immunohistochemical labeling for S-100. Error bars = SD. $^{*}p < 0.001$, versus ANA group, $^{\#}p < 0.001$ versus ANA+7, 8-DHF group, and $^{\triangle}p < 0.01$ versus ANA+BMSCs group. Data were analyzed with a one-way ANOVA followed by Tukey's post hoc test. Scale bars = 100 μm or 20 μm (boxed area).

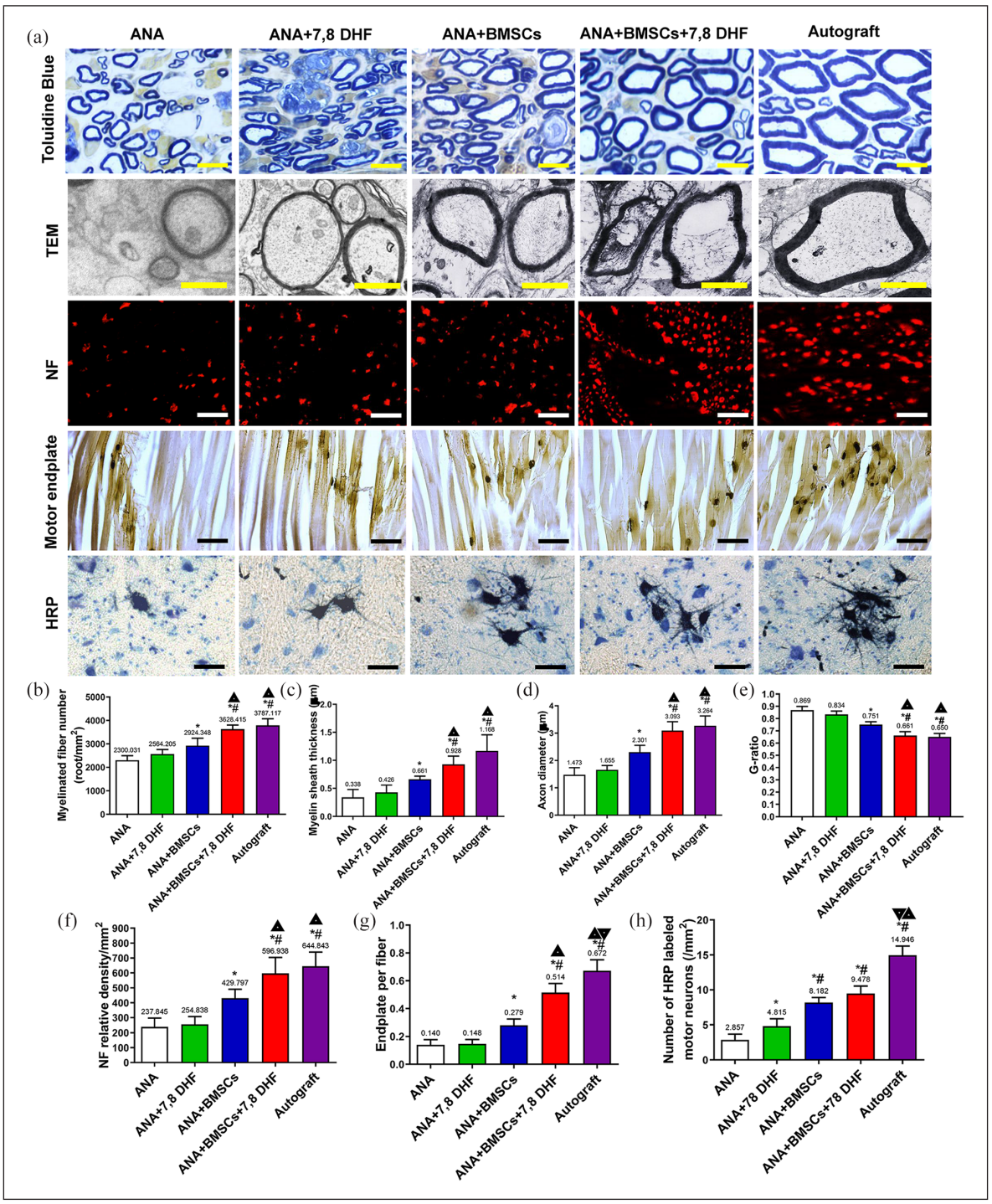

Figure 7. 7, 8-DHF+BMSCs promoted axonal myelination and regeneration in engrafted ANAs, and increased the number of target muscle motor endplates. (a) Histologic photomicrographs of toluidine blue staining, and transmission electron microscope (TEM) analysis of axon and myelinated fibers in regenerating ANAs of the five treatment groups. Representative immunofluorescent images for neurofilament (NF) labeling (red) in cross sections at the center of ANAs; Images show the motor end plate in a longitudinal section of TA muscle from the injured side. Retrograde HRP labeling of ipsilateral L3-L5 ventral horn motor neurons from TA muscles was used to evaluate motor axon regeneration. Images show HRP-labeled ventral horn motor neurons from each treatment group. Quantification of myelinated fiber number (b), myelin sheath thickness (c), axon diameter (d), G-ratio (e) and NF protein expression (f) in the center of the ANAs, the motor end plate number per TA muscle fiber (g) and number of HRP-labeled motor neurons detected in the L3-L5 spinal cord (h) are shown ($n=8$). Error bars = SD. $^{*}p<0.01$, versus ANA group, $^{\#}p<0.05$ versus ANA+7, 8-DHF group, and $^{\triangle}p<0.01$ versus ANA+BMSCs group, $^{\triangledown}p<0.01$ versus ANA+BMSCs+7, 8-DHF group. Data were analyzed with a one-way ANOVA followed by Tukey's post hoc test. Scale bars = 20 μm, 2 μm (TEM), 100 μm (HRP).

groups. Also, motor endplates were significantly decreased in the ANA+BMSCs group compared with the ANA+BMSCs+7, 8-DHF group, and there were increased endplate numbers in the autograft group compared with ANA+BMSCs+7, 8-DHF group ($F_{4,35}=72.90, p<0.001$) (Figure 7(g)). The results strongly indicate a significant positive influence of 7, 8-DHF on neuromuscular motor endplates following engraftment of a BMSC-embedded ANA to repair the sciatic nerve.

HRP-labeled motor neurons were significantly increased in the other treatment groups in comparison to the ANA-only group (Figure 7(a)). Also, HRP+ motor neurons in the ANA+BMSCs+7, 8-DHF and ANA+BMSCs groups were increased compared to the ANA+ 7, 8-DHF group. Motor neuron were also increased in the autograft group compared to the ANA+BMSCs+7, 8-DHF group; however, no significant difference was identified between the ANA+BMSCs+7, 8-DHF and ANA+BMSCs groups ($F_{4,35}=84.18, p<0.001$) (Figure 7(h)). Our results showed that 7, 8-DHF+BMSCs promoted reinnervation of TA muscle post-injury and repair.

The combination 7, 8-DHF+BMSCs significantly upregulated BDNF and TrkB expression, as well as ERK1/2 phosphorylation in regenerating ANA and spinal cord

To elucidate a possible mechanism of treatment by 7, 8 DHF+BMSCs in nerve regeneration, we assessed expression of the TrkB, p-ERK1/2, t-ERK1/2 in ANA tissues (Figure 8(a)). The ANA+BMSCs+7, 8 DHF, ANA+BMSCs and ANA+7, 8-DHF groups exhibited a dramatic increase in TrkB and p-ERK1/2/t-ERK1/2 expression in the graft in comparison to the ANA-only group. Particularly, TrkB and p-ERK1/2/t-ERK1/2 expression in the ANA+7, 8 DHF group and ANA+BMSCs+7, 8-DHF group was significantly upregulated compared to the ANA+BMSCs group, and there were increased TrkB and p-ERK1/2/total-ERK1/2 expression in the ANA+BMSCs+7, 8-DHF group compared with ANA+7, 8 DHF group, however, no significant differences in TrkB and p-ERK1/2/total-ERK1/2 between the ANA and Autograft groups (TrkB: $F_{4,10}=45.77$, $p<0.0001$; p-ERK1/2/t-ERK1/2: $F_{4,10}=95.85$, $p<0.001$) (Figure 8(b) and (c)). Additionally, BDNF expression in secretions was increased in the ANA+BMSCs and ANA+BMSCs+7, 8-DHF groups compared to the ANA, ANA+7, 8 DHF and Autograft groups, however, no significant difference in BDNF expression was observed between the ANA+BMSCs and ANA+BMSCs+7, 8-DHF groups ($F_{4,10}=14.54$, $p<0.0001$) (Figure 8(d)).

Next, we assessed BDNF and TrkB expression in the L3-5 ventral horn of spinal cord tissues. The results of immunofluorescence staining showed that BDNF and TrkB were located in the cytoplasm of motor neurons in the anterior horn of the spinal cord (Figure 9(a)). The number of BDNF or TrkB-positive neurons in the spinal cord were similar to expression patterns observed in the different groups (BDNF: $F_{4,20}=84.24, p<0.001$; TrkB: $F_{4,20}=138.3$, $p<0.001$) (Figure 9(b) and (c))

These results indicate that injured nerve repair using ANA grafts injected with 7, 8-DHF+BMSCs upregulates TrkB levels in the ANA and spinal cord in addition to p-ERK1/2/t-ERK1/2 phosphorylation in regenerating ANAs. We believe 7, 8 DHF+BMSCs can promote axonal myelination though strengthening the survival of BMSCs by stimulates TrkB and the downstream ERK phosphorylation signaling pathway in ANA and spinal cord.

7, 8-DHF+BMSCs significantly improves motor functional recovery of regenerating ANAs

Electrophysiology was utilized to assess neuromuscular integrity and nerve conductance. This analysis was represented using the CMAP index. CMAP amplitude is dependent on the number of innervated muscle fibers. Latency to onset of action potentials indicated the extent of myelination and axon size (Figure 10(a)). Six weeks post-surgery, CMAP values were significantly increased in several groups compared to the ANA group. Such values in the ANA+BMSCs+7, 8-DHF group were significantly increased in comparison to the ANA+BMSCs and ANA+7, 8-DHF group. Furthermore, CMAP levels in the ANA+BMSCs group were significantly increased compared to the ANA+7, 8-DHF group. CMAP in the autograft was significantly increased in comparison to that observed in the ANA+BMSCs+7, 8-DHF group ($F_{4,35}=1171$, $p<0.001$) (Figure 10(b)). Meanwhile, the latency period in the ANA+BMSCs+7, 8 DHF and ANA+BMSCs groups was significantly downregulated compared to the ANA group and ANA+7, 8-DHF group. Furthermore, the latency period in the ANA+BMSCs+7, 8 DHF was decreased compared to the ANA+BMSCs groups. In addition, no significant difference in the latency period was observed between the Autograft and ANA+BMSCs+7, 8-DHF groups ($F_{4,35}=117.8, p<0.001$) (Figure 10(c)).

Next, sciatic nerve function was assessed using the sciatic function index (SFI). At 28, 35, 42 days post-surgery, SFI value was markedly increased in other groups compared with the ANA and ANA+ 7, 8-DHF groups. The SFI score in the ANA+BMSCs+7, 8-DHF group was significantly increased compared to the ANA+BMSCs group, and was comparable to the autograft group. No significant difference was observed between the ANA and ANA+ 7, 8-DHF groups (28 days: $F_{4,35}=33.77$, $p<0.001$; 35 days: $F_{4,35}=53.02$, $p<0.001$; 42 days: $F_{4,35}=34.69$, $p<0.001$) (Figure 10(d)). These data demonstrate that 7, 8-DHF+BMSCs promotes significant benefits for improving motor function recovery.

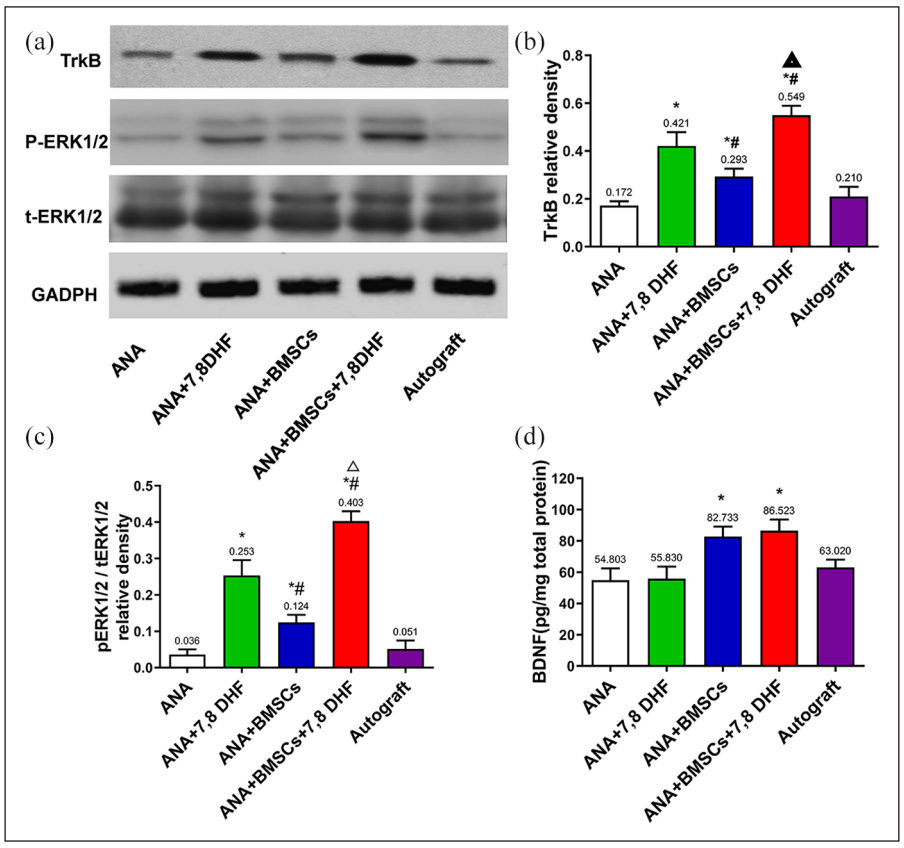

Figure 8. 7, 8-DHF+BMSCs significantly increased BDNF and TrkB expression, as well as Erk phosphorylation in regenerating ANAs. (a) Representative Western blots of TrkB, p-ERK1/2 and t-ERK1/2 expression in harvested ANA tissues from the five treatment groups 28 days post-injury. Error bars = SD. Graphs from the respective analyses represent the relative density of TrkB, p-ERK1/2/t-ERK1/2 protein expression (b, c). ELISA analysis determined BDNF levels secreted from harvested ANA tissues in the five treatment groups (d). The experiment was repeated three times. $^{*}p < 0.01$, versus ANA group, $^{\#}p < 0.01$ versus ANA+7, 8-DHF group, and $^{\triangle}p < 0.01$ versus ANA+BMSCs group. Data were analyzed with a one-way ANOVA followed by Tukey's post hoc test.

Discussion

In the present study, we confirmed that a combination of 7, 8-DHF and BMSC injections into ANAs promote enhanced sciatic nerve regeneration and motor function recovery. This is the first study combining these two treatment approaches for enhancing outcomes following nerve graft in effort to repair the transected peripheral nerve. It is now well accepted that acellular nerve allografts (ANA) are an effective surgical approach for the repair of damaged peripheral nerves. However, there are still limitations that impede complete axon regeneration and optimal target muscle innervation, which has major implications for the extent of functional recovery following nerve engraftment.

In our recent study, BMSCs engineered to overexpress Krüppel-like Factor 7 (KLF7) improved axon regeneration and repair of the injured nerve when injected into an ANA for engraftment into the injured nerve[3] and KLF7 also promotes such benefits in central nervous system injury.[34–36] Prior to this, we found that Schwann cells transfected to over express KLF7, and KLF7 in general, also imparted benefits for successful repair and regeneration of the sciatic nerve following engraftment.[34,35] Through our studies, and those of others, the mechanism by which KLF7 promoted these benefits likely involved increased neurotrophic factor expression, growth cone formation, and axonal myelination.[35] The small-molecule, 7, 8-DHF, is a TrkB agonist also known to promote axon regeneration following peripheral nerve injury,[15] as well as neurite extension and neuroprotection in models of central nervous system injury.[24,28,37] As we found that BDNF was one of the key neurotrophic factors that influenced nerve repair and axon regeneration in our prior studies, it was logical to test the efficacy of 7, 8-DHF in our model of sciatic nerve allograft in combination with BMSCs engraftment.

After confirming our successful isolation and culture of BMSCs in vitro, we proceeded with testing whether 7, 8-DHF would act on BMSCs through the anticipated TrkB mediated mechanism. Since 7, 8-DHF is a TrkB agonist, we then confirmed that the small molecule stimulated signaling via TrkB in BMSCs in vitro. However, it remains

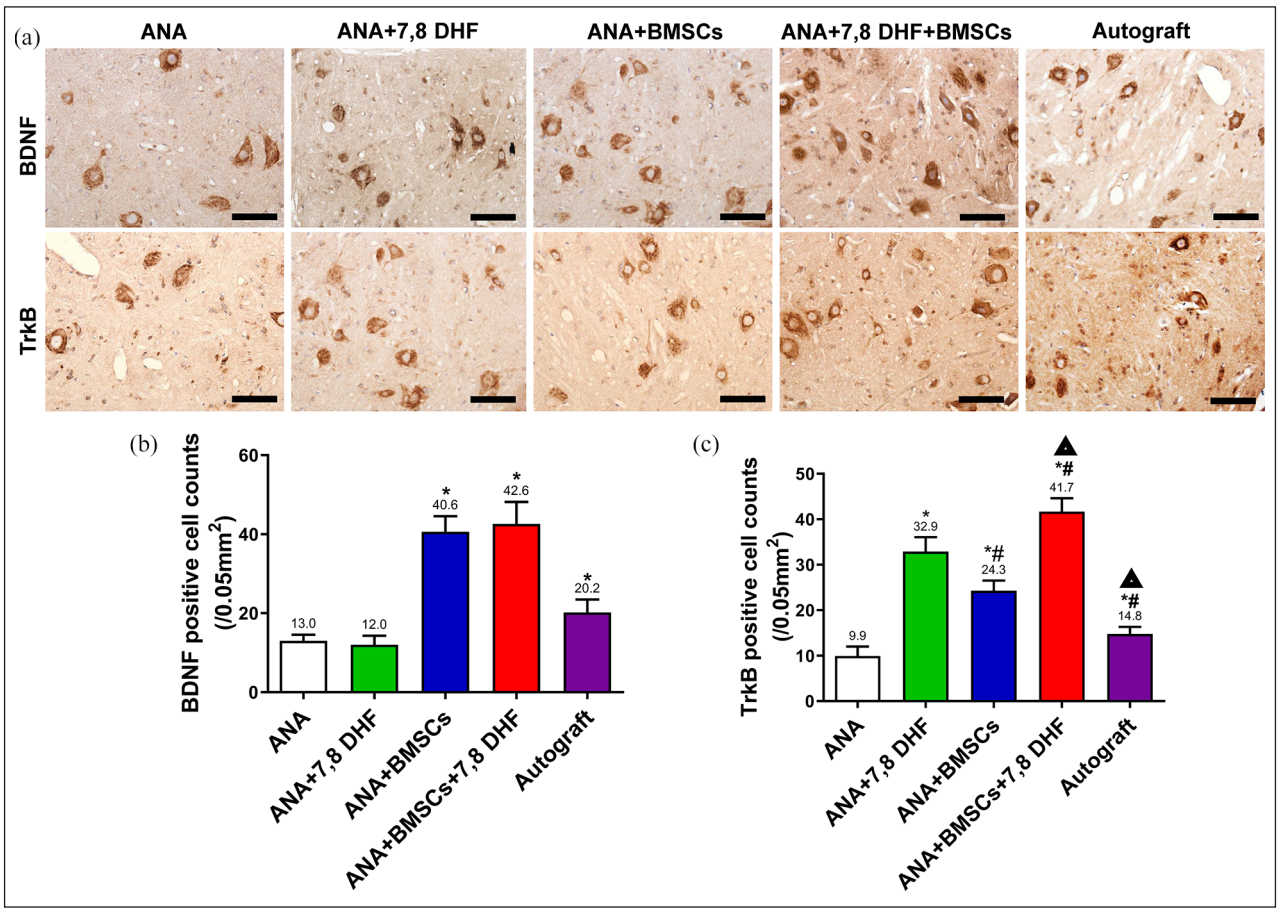

Figure 9. 7, 8-DHF+BMSCs enhanced expression of BDNF and TrkB in ventral horn neurons of the spinal cord. Representative immunohistochemical labeling for BDNF and TrkB in the L3-L5 region ipsilateral to the side of surgery (a). Quantification of the number of BDNF or TrkB-labeled neurons in the L3-L5 spinal cord ventral horn (b, c) from each group ($n = 5$). Error bars = SD. $^{*}p < 0.01$, versus ANA group, $^{\#}p < 0.01$ versus ANA+7, 8-DHF group, and $^{\triangle}p < 0.01$ versus ANA+BMSCs group. Data were analyzed with a one-way ANOVA followed by Tukey's post hoc test. Bars = 200 μm.

unclear whether 7, 8-DHF affects BDNF expression. Our results show that 7, 8-DHF does not increase BDNF secretion levels in BMSCs and 7, 8-DHF mimics several BDNF functions; however, at present 7, 8-DHF does not seem able to influence BDNF secretion in BMSCs. However, 7, 8 DHF can bind to the TrkB receptor and activate downstream signaling elements in a manner similar to that produce by BDNF, and the activation of TrkB receptor pathway results in the activation of Erk1/2. This was confirmed via observation that 7, 8-DHF activates ERK1/2 signaling pathway via TrkB activation instead of promoting BDNF secretion.[38] A recent study on the effects of 7, 8-DHF treatment on TrkB and downstream signaling in an experimental model of intracerebral hemorrhage confirmed our result that 7, 8-DHF promoted Akt phosphorylation through TrkB activation, which was associated with a neuroprotective effect of the drug in that injury model.[39] However, Erk1/2 was phosphorylation was not enhanced by 7, 8-DHF. These results corroborated findings observed in a traumatic brain injury study[38] as well as an in vitro motor neuron neuroprotection study[40] involving 7, 8-DHF as a therapy. On the contrary, 7, 8-DHF promoted neuroprotection in a hypoxia-ischemia retinal injury model via TrkB and Erk1/2 phosphorylation and activation which involved Muller glial cell regeneration.[41] It has been suggested that BDNF-mediated TrkB and Erk1/2 activation regulates IL-6 production among other cytokines in BMSCs,[42] so perhaps the mechanisms of TrkB activation by 7, 8-DHF in BMSCs in our study, and the resultant Erk1/2 phosphorylation, is cell type dependent. Enhancement of Erk activity is associated with promotion of cell proliferation, survival, and differentiation. These effects were mostly blocked by application of U0126, which we observed in BMSCs in vitro following 7, 8-DHF treatment, which provides some explanation for the involvement of MAPK signaling post-treatment in BMSCs. Since the greatest elevation of these signaling pathways was observed both in the graft and in the lumbar spinal cord, this indicates that the peripheral ANA with BMSCs and 7, 8-DHF stimulated a physiologic response

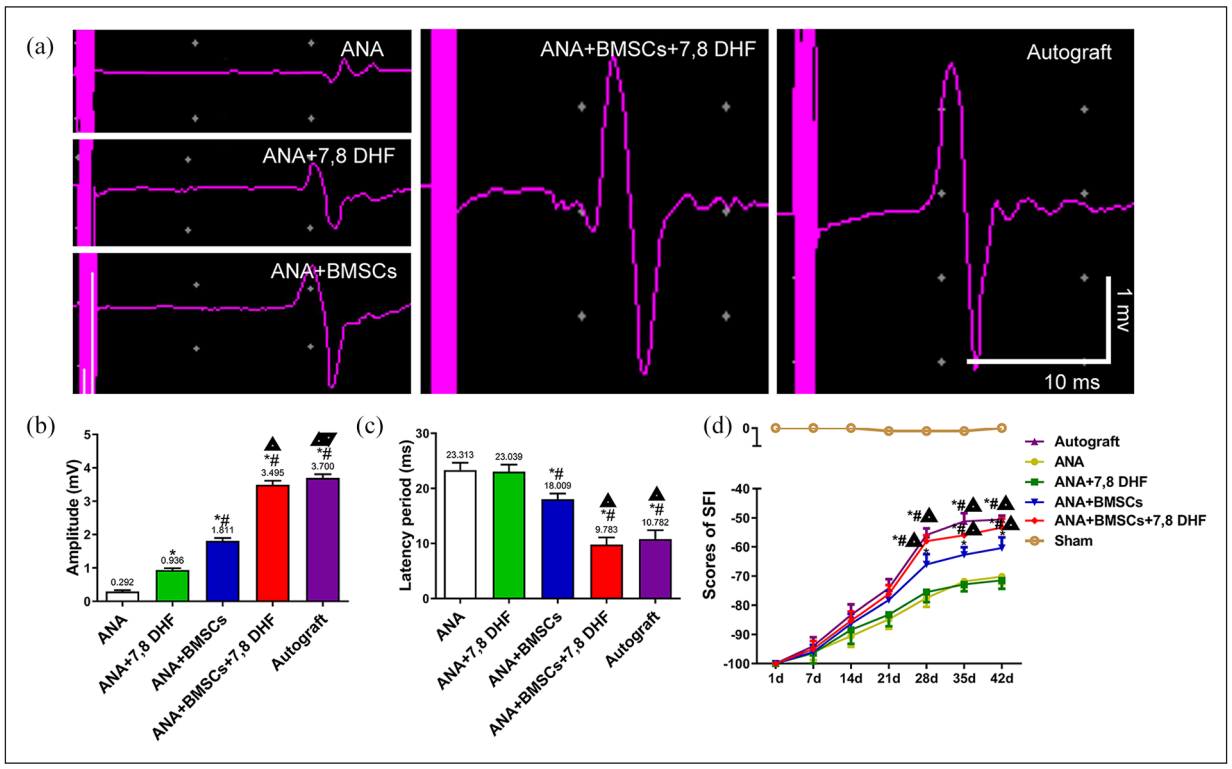

Figure 10. 7, 8-DHF+BMSCs significantly improved recovery of motor function and regenerating ANAs. Electrophysiological index (a), including the compound action potential amplitude (CAMP) (mV) and (b) latency (ms) (c) in ANAs from each treatment group 6 weeks after surgery ($n = 8$). Analysis of the sciatic function index (SFI) (d), and Error bars = SD. *$p < 0.01$, versus ANA group, #$p < 0.01$ versus ANA+7, 8-DHF group, $^{\triangle}p < 0.01$ versus ANA+BMSCs group. Data were analyzed with a one-way ANOVA followed by Tukey's post hoc test.

of neurons in the spinal cord. However, if cytokine production is a key outcome of Erk1/2 phosphorylation in our study, further research is necessary to clarify why and how this response is important for the observed beneficial results in our nerve injury and repair model.

Our findings that 7, 8-DHF promoted BMSCs survival and proliferation in vitro helps explain why we saw increased transplanted BMSC in the ANA of the 7, 8-DHF+BMSC group. This is important, as cellular survival is always a concern in studies involving transplantation of cells into a new environment. However, few differentiated cells with double labeling of PKH26 and S100 was observed in the ANA in two BMSCs transplantation groups. This confirmed minimal differentiation of BMSCs to Schwann-like cells in vivo, which suggested that BMSC-mediated induction may not have been a major contributor to myelinated axon regeneration in our study. Furthermore, this effect may be attributable to the production of neurotrophic factors by BMSCs.[3] Since we know that BMSCs promote axonal growth and myelination in ANAs from our previous research,[3] this observed positive influence of 7, 8-DHF on the engrafted BMSCs in ANAs in this study suggested enhanced this effect over BMSC engraftment into ANAs alone. This is in fact what we observed. We measured myelination through S100 labeling and light and electron microscopy and found that ANA +7, 8-DHF+BMSCs enhanced the number of myelinated fibers, myelin thickness, and G-ratio over ANA+BMSCs alone. We also found that axon number was increased in this combination treatment group. As in previous studies,[43,44] the G-ratio following BDNF treatment of regenerating nerve was greatest in the 7, 8-DHF group. However, the myelinated axons and myelin thickness following BDNF treatment in those studies were similar to those in the 7, 8-DHF group in present study. The primary rationale and explanation for this phenomenon is that the time point we observed was earlier than those in previous studies. Moreover, the SFI value of 7, 8-DHF group in our study was superior to that of BDNF + PLGA group at 4 weeks after surgery in another previous study.[45] These findings indicate that 7, 8-DHF enhances myelin regeneration as well as functional recovery, and serve as an alternative to BDNF.

Based on our results showing influence on cell replication and viability, it seems likely that 7, 8-DHF could be modulating Schwann cell survival in the ANA, secretion of regeneration-promoting trophic factors, and production of myelin which would improve conduction of signals through the newly regenerated axons. BDNF is known to promote such outcomes in Schwann cells and injured

peripheral nerve and axons, and that this effect was found to be mediated through upregulation of the purinergic P2X4 receptor (P2X4R) on Schwann cells and in the injured peripheral nerve.[46] This upregulation in Schwann cells was shown to promote motor axon regeneration and Schwann cell myelination through promoting upregulated BDNF secretion by affected Schwann cells. As 7, 8-DHF acts similarly to BDNF, perhaps 7, 8-DHF acts directly on Schwann cells to promote these reparative benefits. It could also be a result of increased BDNF secretion by BMSCs exposed to 7, 8-DHF. As the possible cellular and molecular mechanisms by which the benefits are observed are numerous, it is likely that the TrkB agonist affects various cells and components in and around the ANA to promote the regenerative and myelination benefits documented in the present study.

Looking distally to the neuromuscular interface and sciatic functional index analyses, the results support the potentially Schwann cells mediated influence on regenerating axons and myelination, and possibly through effects on BMSCs in the ANA+7, 8-DHF+BMSCs treatment, as ANA+7, 8-DHF alone does not achieve the same positive results. We found that in the ANA+7, 8-DHF+BMSCs treatment group, motor endplates were significantly increased over all other treatment groups, as well as SFI scores over time. We also saw through retrograde labeling of the motor neuron soma that soma size dendritic arbor was increased in response to the ANA+7, 8-DHF+BMSCs treatment of the injured sciatic nerve. As BDNF is known to promote motor neuron survival and ameliorate degenerative effects on motor neurons,[47,48] it may be that increased BDNF secretion by Schwann cells or BMSCs acted on regenerating neurons to induce protection or regeneration in the motor neuron soma. If this is possible, then it is also possible that 7, 8-DHF was directly triggering this effect or it is a combination of both BDNF and 7, 8-DHF that is required for these central neuronal benefits from a peripheral treatment. Our previous report[49] demonstrated retrogradely transported NT-3 from sciatic nerve could remodel lumbar neural circuitry after thoracic spinal cord injury (SCI). We hypothesized that 7, 8-DHF or/and BDNF treatment of the sciatic nerve led to the retrograde transportation of TrkB to the lumbar motor neurons (MNs), resulting in increased TrkB-mediated signaling in the MNs, lumbar MNs dendritic regrowth, and promote MNs survival following SCI. Additional research is necessary to help elucidate exactly how the ANA+7, 8-DHF+BMSC group exhibited such beneficial effects, though our findings indicate BDNF and TrkB upregulation by motor neurons in the lumbar spinal cord in response to the combination treatment ANA graft is a possible mechanism.

Conclusion

The administration of both BMSCs and the TrkB agonist, 7, 8-DHF into an acellular nerve allograft prior to its engraftment showed promising therapeutic effects through enhancing regeneration and myelination in injured sciatic nerve. In addition, neuromuscular innervation and functional outcomes were also improved by this combination therapy compared to other treatments in our study. We believe the present study establishes a foundation for further mechanistic investigations into how the treatments promoted specific outcomes, and also, how to modulate the combination of BMSCs and 7, 8-DHF in an ANA for optimal regeneration and recovery following nerve graft repair of the injured sciatic nerve. This study is limited as it did not elucidate long-term functional recovery role (ie, 8 weeks, 12 weeks) of combined treatment in vivo after PNI, which requires further investigation.

Declaration of conflicting interests

The author(s) declared no potential conflicts of interest with respect to the research, authorship, and/or publication of this article.

Funding

The author(s) disclosed receipt of the following financial support for the research, authorship, and/or publication of this article: This study was supported by the Science Fund Project of Natural Science Foundation of China (81870977, 81973317,U1903124); Natural Science Foundation of Heilongjiang, China (H2018068), the Basic Research Operating Expenses Program of Heilongjiang provincial Universities (2019-KYYWFMY-0018), Graduate Innovative Research Projects of Mudanjiang Medical College(2019YJSCX-06MY, YJSCX-22MY), Ningxia High School first-class Disciplines (West China first-class Disciplines Basic Medical Sciences at Ningxia Medical University) (NXYLXK2017B07), the Natural Science Foundation of Ningxia Province (2018AAC03067).

Ethical approval

This study was approved by the Animal Care and Use Committee of China Medical University.

Statement of human and animal rights

All of the experimental procedures involving animals were performed in accordance with the Institutional of Health Guide for the Care and Use of Laboratory Animals of China Medical University and approved by the Animal Care and Use Committee of China Medical University.

Informed consent

There are no human subjects in this article and informed consent is not applicable.

ORCID iD

Ying Wang https://orcid.org/0000-0003-4075-781X

References

1. Jia H, Wang Y, Chen J, et al. Combination of BMSCs-laden acellular nerve xenografts transplantation and G-CSF

administration promotes sciatic nerve regeneration. *Synapse* 2019; 73(7): e22093.
2. Wang Y, Jia H, Li WY, et al. Synergistic effects of bone mesenchymal stem cells and chondroitinase ABC on nerve regeneration after acellular nerve allograft in rats. *Cell Mol Neurobiol* 2012; 32(3): 361–371.
3. Li W, Zhu GY, Yue W, et al. KLF7 overexpression in bone marrow stromal stem cells graft transplantation promotes sciatic nerve regeneration. *J Neural Eng*. 2019; 16(5): 056011.
4. Wang Y, Jia H, Li WY, et al. Molecular examination of bone marrow stromal cells and chondroitinase ABC-assisted acellular nerve allograft for peripheral nerve regeneration. *Exp Ther Med* 2016; 12(4): 1980–1992.
5. Wilhelm JC, Xu M, Cucoranu D, et al. Cooperative roles of BDNF expression in neurons and Schwann cells are modulated by exercise to facilitate nerve regeneration. *J Neurosci* 2012; 32(14): 5002–5009.
6. English AW, Meador W and Carrasco DI. Neurotrophin-4/5 is required for the early growth of regenerating axons in peripheral nerves. *Eur J Neurosci* 2005; 21(10): 2624–2634.
7. Poduslo JF and Curran GL. Permeability at the blood-brain and blood-nerve barriers of the neurotrophic factors: NGF, CNTF, NT-3, BDNF. *Brain Res Mol Brain Res* 1996; 36(2): 280–286.
8. Poduslo JF, Curran GL and Berg CT. Macromolecular permeability across the blood-nerve and blood-brain barriers. *Proc Natl Acad Sci USA* 1994; 91(12): 5705–5709.
9. Kishino A, Katayama N, Ishige Y, et al. Analysis of effects and pharmacokinetics of subcutaneously administered BDNF. *Neuroreport* 2001; 12(5): 1067–1072.
10. Zhang Z, Liu X, Schroeder JP, et al. 7,8-dihydroxyflavone prevents synaptic loss and memory deficits in a mouse model of Alzheimer's disease. *Neuropsychopharmacology* 2014; 39(3): 638–650.
11. Munson JB, Shelton DL and McMahon SB. Adult mammalian sensory and motor neurons: roles of endogenous neurotrophins and rescue by exogenous neurotrophins after axotomy. *J Neurosci* 1997; 17(1): 470–476.
12. Skaper SD and Walsh FS. Neurotrophic molecules: strategies for designing effective therapeutic molecules in neurodegeneration. *Mol Cell Neurosci* 1998; 12(4–5): 179–193.
13. Geoffroy H and Noble F. BDNF during withdrawal. *Vitam Horm* 2017; 104: 475–496.
14. Thoenen H and Sendtner M. Neurotrophins: from enthusiastic expectations through sobering experiences to rational therapeutic approaches. *Nat Neurosci* 2002; 5 Suppl: 1046–1050.
15. English AW, Liu K, Nicolini JM, et al. Small-molecule trkB agonists promote axon regeneration in cut peripheral nerves. *Proc Natl Acad Sci USA* 2013; 110(40): 16217–16222.
16. Liu X, Chan CB, Jang SW, et al. A synthetic 7,8-dihydroxyflavone derivative promotes neurogenesis and exhibits potent antidepressant effect. *J Med Chem* 2010; 53(23): 8274–8286.
17. Gonzalez-Lara LE, Xu X, Hofstetrova K, et al. The use of cellular magnetic resonance imaging to track the fate of iron-labeled multipotent stromal cells after direct transplantation in a mouse model of spinal cord injury. *Mol Imaging Biol* 2011; 13(4): 702–711.
18. Kajiya M, Takeshita K, Kittaka M, et al. BDNF mimetic compound LM22A-4 regulates cementoblast differentiation via the TrkB-ERK/Akt signaling cascade. *Int Immunopharmacol* 2014; 19(2): 245–252.
19. Wang X, Zhang L, Zhan Y, et al. Contribution of BDNF/TrkB signalling in the rACC to the development of pain-related aversion via activation of ERK in rats with spared nerve injury. *Brain Res* 2017; 1671: 111–120.
20. Okada K, Tanaka H, Temporin K, et al. Methylcobalamin increases Erk1/2 and Akt activities through the methylation cycle and promotes nerve regeneration in a rat sciatic nerve injury model. *Exp Neurol* 2010; 222(2): 191–203.
21. Han XH, Cheng MN, Chen L, et al. 7,8-dihydroxyflavone protects PC12 cells against 6-hydroxydopamine-induced cell death through modulating PI3K/Akt and JNK pathways. *Neurosci Lett* 2014; 581: 85–88.
22. Zhang Y, Qiu B, Wang J, et al. Effects of BDNF-transfected BMSCs on neural functional recovery and synaptophysin expression in rats with cerebral infarction. *Mol Neurobiol* 2017; 54(5): 3813–3824.
23. Ritfeld GJ, Patel A, Chou A, et al. The role of brain-derived neurotrophic factor in bone marrow stromal cell-mediated spinal cord repair. *Cell Transplant* 2015; 24(11): 2209–2220.
24. Chen L, Gao X, Zhao S, et al. The small-molecule TrkB agonist 7, 8-dihydroxyflavone decreases hippocampal newborn neuron death after traumatic brain injury. *J Neuropathol Exp Neurol* 2015; 74(6): 557–567.
25. Liu NK, Zhang YP, Titsworth WL, et al. A novel role of phospholipase A2 in mediating spinal cord secondary injury. *Ann Neurol* 2006;59(4): 606–619.
26. Khanmohammadi N, Sameni HR, Mohammadi M, et al. Effect of transplantation of bone marrow stromal cell- conditioned medium on ovarian function, morphology and cell death in cyclophosphamide-treated rats. *Cell J* 2018; 20(1): 10–18.
27. Wang Y, Li WY, Jia H, et al. KLF7-transfected Schwann cell graft transplantation promotes sciatic nerve regeneration. *Neuroscience* 2017; 340: 319–332.
28. Zhao S, Gao X, Dong W, et al. The role of 7,8-dihydroxyflavone in preventing dendrite degeneration in cortex after moderate traumatic brain injury. *Mol Neurobiol* 2016; 53(3): 1884–1895.
29. Byers JS, Huguenard AL, Kuruppu D, et al. Neuroprotective effects of testosterone on motoneuron and muscle morphology following spinal cord injury. *J Comp Neurol* 2012; 520(12): 2683–2696.
30. Jia H, Wang Y, Tong XJ, et al. Sciatic nerve repair by acellular nerve xenografts implanted with BMSCs in rats xenograft combined with BMSCs. *Synapse* 2012; 66(3): 256–269.
31. Sengelaub DR and Xu XM. Protective effects of gonadal hormones on spinal motoneurons following spinal cord injury. *Neural Regen Res* 2018; 13(6): 971–976.
32. Yang Y, Ding F, Wu J, et al. Development and evaluation of silk fibroin-based nerve grafts used for peripheral nerve regeneration. *Biomaterials* 2007; 28(36): 5526–5535.
33. de Medinaceli L, Freed WJ and Wyatt RJ. An index of the functional condition of rat sciatic nerve based on measurements made from walking tracks. *Exp Neurol* 1982; 77(3): 634–643.

34. Li WY, Zhang WT, Cheng YX, et al. Inhibition of KLF7-targeting microRNA 146b promotes sciatic nerve regeneration. *Neurosci Bull* 2018; 34(3): 419–437.
35. Wang Z, Winsor K, Nienhaus C, et al. Combined chondroitinase and KLF7 expression reduce net retraction of sensory and CST axons from sites of spinal injury. *Neurobiol Dis* 2017; 99: 24–35.
36. Li WY, Wang Y, Zhai FG, et al. AAV-KLF7 promotes descending propriospinal neuron axonal plasticity after spinal cord injury. *Neural Plast* 2017; 2017: 1621629.
37. Zhao S, Yu A, Wang X, et al. Post-injury treatment of 7,8-dihydroxyflavone promotes neurogenesis in the hippocampus of the adult mouse. *J Neurotrauma* 2016; 33(22): 2055–2064.
38. Wu CH, Hung TH, Chen CC, et al. Post-injury treatment with 7,8-dihydroxyflavone, a TrkB receptor agonist, protects against experimental traumatic brain injury via PI3K/Akt signaling. *PLoS One* 2014; 9(11): e113397.
39. Wu CH, Chen CC, Hung TH, et al. Activation of TrkB/Akt signaling by a TrkB receptor agonist improves long-term histological and functional outcomes in experimental intracerebral hemorrhage. *J Biomed Sci* 2019; 26(1): 53.
40. Tsai T, Klausmeyer A, Conrad R, et al. 7,8-Dihydroxyflavone leads to survival of cultured embryonic motoneurons by activating intracellular signaling pathways. *Mol Cell Neurosci* 2013; 56: 18–28.
41. Huang HM, Huang CC, Tsai MH, et al. Systemic 7,8-dihydroxyflavone treatment protects immature retinas against hypoxic-ischemic injury via muller glia regeneration and MAPK/ERK activation. *Invest Ophthalmol Vis Sci* 2018; 59(7): 3124–3135.
42. Rezaee F, Rellick SL, Piedimonte G, et al. Neurotrophins regulate bone marrow stromal cell IL-6 expression through the MAPK pathway. *PLoS One* 2010; 5(3): e9690.
43. Fu KY, Dai LG, Chiu IM, et al. Sciatic nerve regeneration by microporous nerve conduits seeded with glial cell line-derived neurotrophic factor or brain-derived neurotrophic factor gene transfected neural stem cells. *Artif Organs* 2011; 35(4): 363–372.
44. Alrashdan MS, Sung MA, Kwon YK, et al. Effects of combining electrical stimulation with BDNF gene transfer on the regeneration of crushed rat sciatic nerve. *Acta Neurochir (Wien)* 2011; 153(10): 2021–2029.
45. Zhang Q, Wu P, Chen F, et al. Brain derived neurotrophic factor and glial cell line-derived neurotrophic factor-transfected bone mesenchymal stem cells for the repair of periphery nerve injury. *Front Bioeng Biotechnol* 2020; 8: 874.
46. Su WF, Wu F, Jin ZH, et al. Overexpression of P2X4 receptor in Schwann cells promotes motor and sensory functional recovery and remyelination via BDNF secretion after nerve injury. *Glia* 2019; 67(1): 78–90.
47. Sendtner M, Holtmann B, Kolbeck R, et al. Brain-derived neurotrophic factor prevents the death of motoneurons in newborn rats after nerve section. *Nature* 1992; 360(6406): 757–759.
48. Schabitz WR, Sommer C, Zoder W, et al. Intravenous brain-derived neurotrophic factor reduces infarct size and counterregulates Bax and Bcl-2 expression after temporary focal cerebral ischemia. *Stroke* 2000; 31(9): 2212–2217.
49. Wang Y, Wu W, Wu X, et al. Remodeling of lumbar motor circuitry remote to a thoracic spinal cord injury promotes locomotor recovery. *Elife* 2018; 7: e39016.